Article

Archicarbons: New Carbon Allotropes Build from Circular Arches of Carbon Atoms as Building Blocks

Fabio J. F. S. Henrique, [a] Felipe L. Oliveira [a] and Pierre M. Esteves [*,a]

aInstituto de Química, Universidade Federal do Rio de Janeiro, Av. Athos da, Silveira Ramos, 149, CT, A-629, Cidade Universitária, 21941-909 Rio de Janeiro-RJ, Brazil

Molecular and periodic allotropes based on cyclo[18]carbon, known as archicarbons, were investigated using density functional theory (DFT) in both molecular and periodic models. This study explores the physicochemical characteristics of these exquisite carbon allotropes, including various molecular archicarbons (spiro[18]carbon, bicyclo[8]carbon, 0-tricyclo[8]carbon, 0-bi(cyclo[19]carbon), 1-bi(cyclo[19]carbon), and 0-fused[18]carbon) and periodic archicarbons (poly-spiro[8]carbon, poly-0-bi(cyclo[8]carbon), poly-1-bi(cyclo[8]carbon)). Most proposed molecular archicarbons showed higher cohesive energy than cyclo[18]carbon, except for bicyclo[8]carbon, which suggests that those may be experimentally observable. Proposed synthetic routes for both molecular and periodic archicarbons are suggested, highlighting their potential, particularly in semiconductor applications, and paving the way for further exploration of their distinct electronic properties.

Keywords: archicarbon, polyynic, carbyne, carbon allotrope, cyclo[18]carbon

Introduction

The study of carbon-based structures has sparked significant scientific and technological advances in recent decades.[1-3] The experimental observation of structures such as fullerenes,[4] carbon nanotubes,[5] and graphene[6] has captured significant interest from both scientific and technological standpoints.[7,8] These materials may exhibit unique physicochemical properties, prompting extensive exploration for potential applications. Notably, this research has led to the Nobel Prizes in 1996 to R. Curl, Kroto, and Smalley[3] for the discovery of fullerenes and in 2010 to Geim and Novoselov[3] for the discovery of graphene. Furthermore, numerous technological breakthroughs resulting from these discoveries have profoundly impacted society.[9,10]

For over half a century, the potential existence of molecules comprised solely of sp-hybridized carbon atoms bonded to form a ring, along with their precise chemical structure, has been the focus of intense debate. Molecules such as C_{18}, or cyclo[18]carbon, a planar monocyclic ring composed of 18 carbon atoms can adopt two structural conformations: a cumulenic form characterized by uniform bond lengths, and a polyynic form featuring bond-length alternation (BLA), as depicted in Figure 1a. The determination of the most stable conformation has been a longstanding topic of scientific debate where different stable conformations are obtained depending on the level of theory employed on the simulations.[11-17] At the heart of this debate lies the discussion involving stabilizing electronic factors, such as aromaticity and double aromaticity,[18,19] possible dimerization,[20] and symmetry breaking attributed to second-order Jahn-Teller distortions and Peierls instability effects.[13,17,21]

However, only in 2019 that the cyclo[18]carbon was successfully synthesized, isolated and its structure was determined through atomic force microscopy, indicating a pathway toward the resolution of this debate showing that it has a polyynic bonding pattern.[22] The discovery of cyclo[18]carbon also marked the beginning of a journey to explore this family of structures further, both computationally and experimentally. Several computational studies focused on exploring the cyclo[n]carbons up to C_{100},[23-25] while members such as cyclo[10]carbon,[26] cyclo[13]carbon,[27] cyclo[14]carbon,[26] cyclo[16]carbon[28] and cyclo[26]carbon[27] have also been observed experimentally, highlighting the importance of the conceptual debate over elusive structures before their experimental realization.

Inspired by the fascinating conceptual debate preceding the experimental realization of the cyclo[*n*]carbon family, in this study we delve into a simple yet intriguing question: how can we push the boundary of structural complexity in molecules comprised exclusively of carbon atoms one step further? To answer this question, here we propose a range of new molecular and 1D-periodic carbon allotropes named archicarbons, constructed from the connection of carbyne arches as illustrated in Figure 1b, and employ density functional theory (DFT) calculations to investigate their stability, structure, and important electronic properties.

Methodology

All calculations were carried out based on density functional theory (DFT). For the molecular structures the Gaussian package[29] was employed, while for the 1D periodic structures the Quantum ESPRESSO[30,31] version 6.8 was used. The different software used here were motivated by the nature of the problem to be tackled. The gaussian basis set approach used in Gaussian package is more suitable for non-periodic systems such as the molecular structures while the plane-wave basis set with periodic boundary conditions as applied in Quantum ESPRESSO is more appropriate for periodic systems.

For the molecular structures, several exchange-correlation functionals were tested to reproduce the structural parameters of the cyclo[18]carbon molecule as obtained by coupled-cluster singles and doubles (CCSD) theory, and among the several functional tested, the M11[32] functional with the D3(BJ) dispersion correction method[33] presented better results describing the cyclo[18]carbon structure in its form polyyne (for more details see Table S1 in the Supplementary Information (SI) section). The geometry optimization and vibrational frequency calculations for the molecular structures were performed using the M11-D3(BJ) functional with a def2-TZVP basis set.

For the periodic 1D structures the Perdew-Burke-Ernzerhof (PBE) functional[34] with D3 corrections and ultrasoft pseudopotentials[35] was used to describe the core electrons. The Kohn-Sham orbitals are expanded in a plane-wave basis set with a kinetic energy cutoff of 80 Ry and 800 Ry for the charge density was used.[11] The first Brillouin Zone integration was performed in a Monkhorst-Pack[36] *k*-point mesh of $1 \times 1 \times 6$ for structures poly-spiro[8]carbon and poly-1-bi(cyclo[8]carbon) and $6 \times 1 \times 1$ for structures poly-0-bi(cyclo[8]carbon) and poly-0-fused[8]carbon. Here, the reciprocal axis was selected to match the periodicity of the structure, being poly-spiro[8]carbon and poly-1-bi(cyclo[8]carbon) periodic along the x-axis and poly-0-bi(cyclo[8]carbon) and poly-0-fused[8]carbon periodic along the z-axis. Both the energy cutoff and the *k*-points grid size were chosen based on systematically checking the convergence with total energy, as presented in SI section. Atomic positions were fully optimized using the Broyden-Fletcher-Goldfarb-Shanno (BFGS) *quasi*-newton minimization algorithm[37] until the Hellmann-Feynman forces acting on the atoms were lower than 10^{-5} Ry Bohr^{-1} and total energy changes less than 10^{-10} Ry.

To simulate an isolated 1D periodic system a fixed slab with a size of 17 Å was used, determined based on convergency tests as presented in the SI section. The band diagram and the projected density of states (pDOS) were calculated in a dense k-points grid of $1 \times 1 \times 24$ for structures poly-spiro[8]carbon and poly-1-bi(cyclo[8]carbon) and $36 \times 1 \times 1$ for structures poly-0-bi(cyclo[8]carbon) and poly-0-fused[8]carbon using the tetrahedron method[38] for occupations. The cohesive energy, E_c, was calculated as

$$E_c = E_{carbon} - \frac{E_{tot}}{n_c} \qquad (1)$$

where E_{tot} is the total energy of the structure, E_{carbon} is the energy of an isolated carbon atom on its ground state ($^3P_0$)
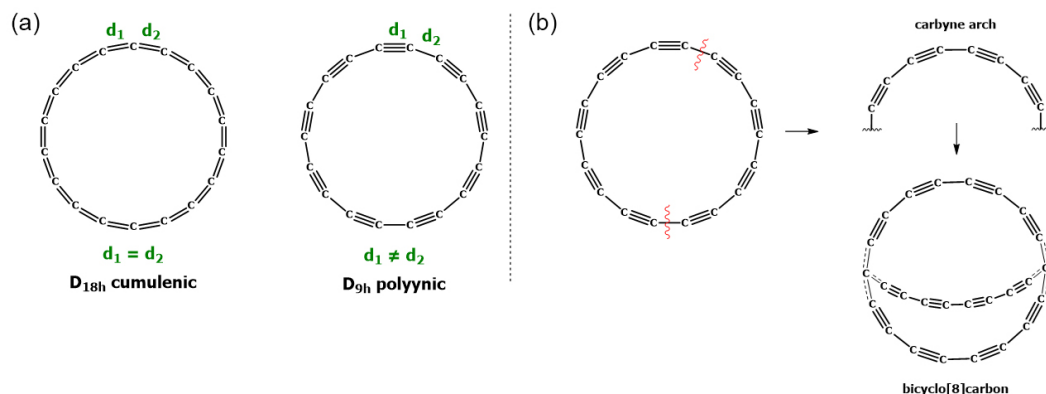

Figure 1. (a) Two possible geometries of C18, or cyclo[18]carbon, highlighting the bond-length alternation that define the cumulenic or polyyinic forms and the structure's point group. (b) Example of strategy for creating the bicyclo[8]carbon using a carbyne arches derived from cyclo[18]carbon.

and n_c is the number of atoms on the structure.

The bond-length alternation (BLA) was calculated as the average of the difference between the N larger (d_{large}) and smaller (d_{small}) bonds (usually associated with single and triple bonds) presented in the carbine arc, as

$$BLA = \frac{1}{N} \sum d_{large} - d_{small} \qquad (2)$$

Phonon dispersions were obtained by diagonalizing the dynamical matrix obtained from the interatomic force constants derived from the finite-displacement method using the PHONOPY software.[39,40] A displacement of 0.01 Å was applied on the cartesian directions for all atoms non-equivalent by symmetry within the unit cell. The interatomic force constants were calculated using a 1 × 1 × 3 supercell for poly-spiro[8]carbon and poly-1-bi(cyclo[8]carbon) and 2 × 1 × 1 supercell for poly-0-bi(cyclo[8]carbon) and poly-0-fused[8]carbon.

Results and Discussion

Molecular allotropes

In an attempt to expand the limits of the structural complexity of molecular carbon allotropes, we first endeavored to systematize a construction logic based on the molecular topology, which represents the connections between atoms and their neighbors, of potential new molecular carbon allotropes. A conceptual framework can be established by considering the structure of cyclo[18]carbon as a carbine section containing 18 carbon atoms forming an arche, with their ends linked to form a single cycle. Building upon this, we can extend the concept to envision two carbine sections with *n* atoms connected through a single sp³-hybridized carbon atom, resulting in the formation of spiro[*n*]carbon (Figure 2a).

Similarly, by connecting three carbine sections containing *n* atoms via carbon atoms, it is possible to create the bicyclo[*n*]carbon molecule (Figure 2b). Further complexity can be achieved by envisaging structures formed from two sets of two arches, each comprising *n* carbon atoms, connected at their ends by single carbon atoms which are in turn linked via carbine sections with *m* carbon atoms, forming bridges between the arches, thereby generating the *m*-tricyclo[*n*]carbon (Figure 2c).

For the *m*-tricyclo[*n*]carbon molecule it is possible to anticipate some structural constraints that may lead to relevant consequences on the stability of the molecule. The most important is that only even values for *m* should result in a stable structure, as odd values would lead to the
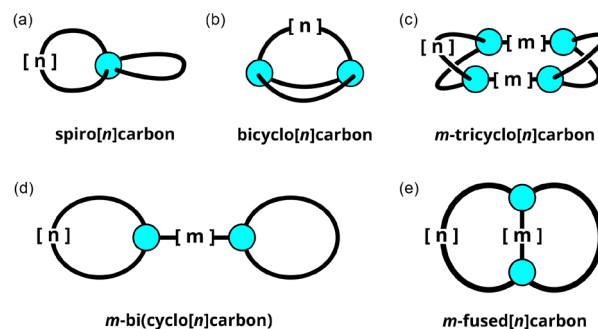

Figure 2. Scheme representing the topology of the new proposed molecular carbon allotropes. The [*m*] and [*n*] represent the number of carbon atoms on the respective sections of each structure while the blue circles represent the carbon atoms that form the connection between the carbine sections.

formation of cumulenic bonds within the carbon bridges which is forbidden by the π-orbitals geometry, thereby generating unstable molecules.

Alternatively, it is possible to consider structures of cyclo[*n*]carbons directly connected through a carbine section with *m* atoms, forming the *m*-bi(cyclo[*n*]carbon) molecule (Figure 2d). Here, the number of *m* carbon atoms will also affect the molecular geometry. When even numbers of *m* carbons are used the *n*-cyclo moieties will be at the same plane, and when odd numbers of *m* carbons are used the *n*-cyclo moieties will be forced to be perpendicular to each other. This may have important impacts on the stability of the molecule and electronic properties.

Finally, if cyclo carbons are fused through two points, so that there are external loops with *n* carbon atoms with an internal bridge with *m* carbon atoms, it is possible to generate the *m*-fused[*n*]carbon molecule (Figure 2e). Analogous to the *m*-tricyclo[*n*]carbon, here the number of *m* carbon atoms within the carbon bridge must be even, as odd numbers will generate a cumulenic arrangement of the π-bonds that is forbidden due to the improper orientation of the π orbitals.

It is important to emphasize that the "construction rules" presented here are not intended to be synthetic routes, but rather a logical pathway for understanding the three-dimensional structure that allows the generalization to create families of molecular carbon allotropes, akin to the cyclo[*n*]carbon family. Some proposed synthetic pathways for selected molecules from each of these families are outlined in subsequent sections and may serve as starting points for future synthetic efforts.

To study the physicochemical characteristics of these proposed families of carbon allotropes, we decided to select a specific member from each family, chosen so that its structure resembles cyclo[18]carbon, which is known to be one of the most stable members of the cyclo[*n*]carbon family. Thus, throughout this work, we will focus

on the molecules spiro[18]carbon, bicyclo[8]carbon, 0-tricyclo[8]carbon, 0-bi(cyclo[19]carbon), 1-bi(cyclo[19]carbon), and 0-fused[18]carbon. Nevertheless, there are no restrictions that systems containing other ring sizes might also be stable, and this will be the subject of future studies.

The optimized geometries for the proposed carbon allotropes with their respective point group symmetry are presented in Figure 3. Vibrational analysis indicates that all structures correspond to a minimum on the potential energy surfaces, as no imaginary frequencies were observed for any of the molecules.

The spiro[18]carbon (Figure 3a) molecule is formed by two carbine arches, each consisting of 18 carbon atoms connected at their ends by one sp^3 carbon atom, thereby forming a *spiro* moiety at the center. This arrangement forces the arches to be perpendicular to each other preventing the π-bonds from being fully conjugated. In fact, when analyzing the characteristics of the highest occupied molecular orbitals (Figure S26, SI section) it is possible to notice that the π-systems are separated by the sp^3 carbon atom. After the geometry optimization, the molecule exhibited D_{2d} point group symmetry, with the arches exhibiting a polyynic conformation. The alternating bonds measure on average 1.36 and 1.21 Å, resulting in a bond-length alternation (BLA) of 0.155 Å, higher than cyclo[18]carbon that presents a BLA of 0.143 Å at the same level of theory.

The bicyclo[8]carbon (Figure 3b) molecule is formed by three arches, each comprised of 8 carbon atoms connected at the ends by two carbon atoms. After the geometry optimization, the molecule presented D_{3h} point group symmetry, with the arches adopting a polyynic conformation, with alternating bonds measures 1.34 and 1.22 Å, resulting in a BLA of 0.119 Å. The carbon atoms connecting the three arches possess sp^2 character, with bond lengths of 1.39 Å and angles between arches measuring 118°.

Now, considering 0-tricyclo[8]carbon, this molecule is generated by linking two carbine sections with 8 carbon atoms through one carbon atom at each end and then, linking this unit directly to an equivalent, generating a molecule with four sets of arches with 8 carbon atoms connected by four carbon atoms. Interestingly, when analyzing the highest occupied molecular orbitals (Figure S25, SI section) it is possible to notice that there is the possibility of conjugation between the arcs of each portion of the molecule. After geometry optimization the molecule showed a D_{2h} point group symmetry with the four arches exhibiting a polyynic conformation, with bond lengths of 1.37 and 1.21 Å, resulting in a BLA of 0.160 Å. The carbon bridges between the sets of two eight-member arches presented a bond length of 1.37 Å, while the bond with the eight-member arches measures 1.43 Å and the angles between the eight-member arches are 114°.

Regarding *m*-bi(cyclo[*n*]carbon), we investigated two alternative scenarios: one with zero carbon atoms between the connections of the cyclical units, named 0-bi(cyclo[19]carbon), and another with one atom between these connections, resulting in 1-bi(cyclo[19]carbon). We chose to study two members of this family due to their distinctive feature: when there is an even number of carbon atoms between the connection of the two cyclical portions, they are joined by a double bond and remain in the same plane. However, when there is an odd number of carbon atoms, the formation of cumulenic double bonds occurs in the connection, causing these units to occupy perpendicular planes.

For the 0-bi(cyclo[19]carbon) (Figure 3d), the geometry optimization yields a molecule with D_{2h} point group symmetry, while the 1-bi(cyclo[19]carbon) (Figure 3e) presented D_{2d} point group symmetry. As expected, the two cyclical portions of 0-bi(cyclo[19]carbon) remained in the same plane, while for 1-bi(cyclo[19]carbon), they were maintained in perfectly perpendicular planes. In both cases, the cyclic moieties exhibited polyynic character,
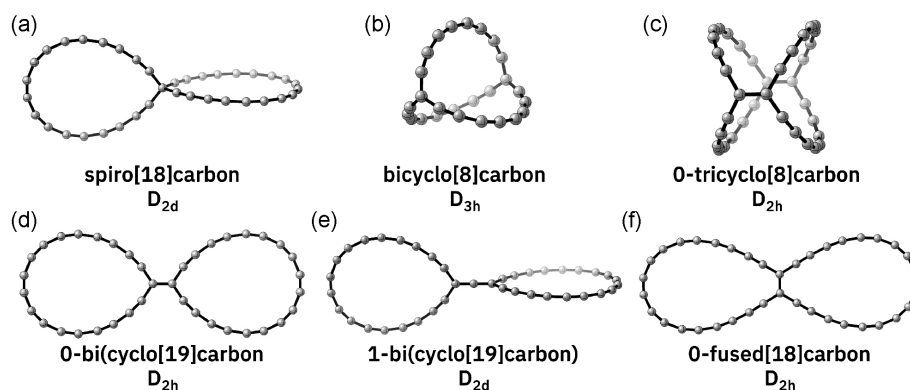

Figure 3. Optimized geometries, point group symmetry, and name of the proposed molecular carbon allotropes.

with bond lengths of approximately 1.36 and 1.21 Å, resulting in a BLA of 0.152 Å for $m = 0$ and 0.154 Å for $m = 1$. For 0-bi(cyclo[19]carbon), the bond connecting the cyclic moieties presented a length of 1.47 Å, while for 1-bi(cyclo[19]carbon), the two bonds showed length of 1.31 Å. In the case of 0-bi(cyclo[19]carbon) (Figure S28, SI section), the π orbitals are found to be fully conjugated along the structure. Conversely, 1-bi(cyclo[19]carbon) (Figure S29, SI section) displays two sets of higher-energy degenerate orbitals, each of which is located in a cyclic moieties of the molecule.

Finally, the 0-fused(cyclo[18]carbon) exhibited D_{2h} point group symmetry after geometry optimization. The carbine arches also displayed polyynic character, with bond lengths of 1.36 and 1.21 Å, resulting in a BLA of 0.154 Å, while the bond connecting the arches presented a length of 1.37 Å. Here, it is also possible to notice that the highest occupied levels (Figure S27) correspond to π orbitals fully conjugated along the structure.

Relative stability and electronic properties

The stability of the proposed allotropes has been evaluated in terms of cohesive energy, i.e., the difference between the energy of an isolated carbon atom and the energy *per* atom of the structure. Table 1 shows the results of this assessment for the newly proposed carbon allotropes compared with the cyclo[18]carbon. It is noteworthy that almost all the presented structures exhibit higher cohesive energy than cyclo[18]carbon, except for bicyclo[8]carbon which exhibits 0.002 eV atom⁻¹ less than cyclo[18]carbon. This result is notably promising, given that cyclo[18]carbon stands as one of the most stable constituents within the cyclo[*n*]carbon family.[23]

Among the structures presented, the 0-fused[18]carbon and the 0-bi(cyclo[19]carbon) exhibited the highest

cohesive energy, at 7.78 and 7.77 eV atom⁻¹, respectively. The elevated stability of these structures may be attributed to the potential for π-bond conjugation between the cyclo portions of the molecules, which enhances electronic delocalization and thus molecular stability. Besides that, these structures presented higher bond-length alternation than cyclo[18]carbon, a characteristic that is directly correlated with molecular stability. Interestingly, 1-bi(cyclo[19]carbon) closely resembles its counterpart 0-bi(cyclo[19]carbon) but with an additional carbon atom between the cyclo portions. Despite that, it is 0.02 eV atom⁻¹ less stable than its parent indicating that the π-conjugation between the cyclic moieties is an important stabilizing factor in these structures.

A similar trend of stability can be observed between 0-tricyclo[8]carbon and spiro[18]carbon, which displayed cohesive energies of 7.76 and 7.73 eV atom⁻¹, respectively. This difference in cohesive energy can also be attributed to the potential for conjugation of π-bonds, which is feasible in the former but not in the latter due to the presence of a sp^3 carbon atom connecting the cyclo portions.

The bicyclo[8]carbon is the only one among the proposed structures that are less stable than the cyclo[18]carbon. However, this observation does not necessarily imply that the synthesis of the molecule in question is unfeasible. Other members of the cyclocarbon family, such as cyclo[10]carbon or cyclo[14]carbon, have been calculated to be less stable than their 18-atom counterparts, nevertheless, they were experimentally observed.

The energy gap (ΔE) between the highest occupied molecular orbital (E_{HOMO}) and the lowest unoccupied molecular orbital (E_{LUMO}) was calculated for all proposed molecular carbon structures and for cyclo[18]carbon applying the M11 and HSE06 functionals and the results are presented in Table 1. In both functionals, it was observed that all proposed molecular structures exhibited a lower ΔE than cyclo[18]carbon.

Analysis of the ΔE obtained from the HSE06 functional, that usually results in ΔE values close to the experimental ones, shows that bicyclo[8]carbon and 0-tricyclo[8]carbon presented ΔE values of 1.90 and 1.19 eV, respectively, considerably lower than cyclo[18]carbon. This could be related to the nature of the conjugation of π-bonds between the eight-carbon arches in each structure, as shown in Figures S24 and S25 (SI section). Similar behavior was verified for 0-fused[18]carbon and 0-bi(cyclo[19]carbon), with ΔE values of 1.55 and 1.97 eV, respectively. In these structures the 18-carbon arches are connected by sp^2 carbons, forming a planar structure, and allowing for π-bond conjugation between the cyclic moieties.

Table 1. Cohesive energy and HOMO-LUMO gap (ΔE) of the new molecular carbon allotropes compared with cyclo[18]carbon

Structure	Cohesive energy / (eV atom⁻¹)	ΔE ($E_{HOMO} - E_{LUMO}$) / eV	
		M11	HSE06[a]
Cyclo[18]carbon	7.69	7.53	3.31
Spiro[18]carbon	7.73	7.12	2.80
Bicyclo[8]carbon	7.69	4.63	1.90
0-Tricyclo[8]carbon	7.76	5.27	1.19
0-Bi(Cyclo[19]carbon)	7.77	5.83	1.97
1-Bi(Cyclo[19]carbon)	7.75	7.12	2.82
0-Fused[18]carbon	7.78	5.57	1.55

[a]Values calculated within the M11 optimized structure. E_{HOMO}: highest occupied molecular orbital; E_{LUMO}: lowest unoccupied molecular orbital.

Interestingly, spiro[18]carbon and 1-bi(cyclo[19]carbon) presented similar ΔE values, 2.80 and 2.82 respectively, being the highest values among the proposed structures. Their structures consist of cyclic moieties in a perpendicular configuration with carbon atoms linking the two cyclic moieties, which prevents interannular π-conjugation disrupting π-bond conjugation throughout the molecule as in the other structures.

Periodic structures

Based on the new molecular carbon allotropes proposed above it is possible to envision several different 1D-periodic structures using a strategy analogous to the one used to generate the molecular allotropes. For example, by repeating the connection pattern used to create the spiro[*n*]carbon, but now on both sides of a carbon arch instead of just one side as in the molecular version, it is possible to generate a 1D-periodic carbon allotrope represented in Figure 4, named poly-spiro[*n*]carbon. The same approach can be applied to the *m*-bi(cyclo[*n*]carbon) and m-fused[*n*]carbon molecules to generate the poly-*m*-bi(cyclo[*n*]carbon) and poly-*m*-fused[*n*]carbon structures.

Regarding poly-*m*-bi(cyclo[*n*]carbon) and poly-*m*-fused[*n*]carbon structures, the same rules that govern their molecular counterparts apply to the *m* number of atoms present on the carbon bridges. Specifically, for the poly-*m*-bi(cyclo[*n*]carbon) structure if *m* is an odd number, then the cyclic moieties will be oriented perpendicular to each other. Conversely, for the poly-*m*-fused[*n*]carbon structure, only even values of *m* are allowed due to orbital geometry.

To focus our studies on periodic structures, we adopted a methodology akin to that employed for molecular allotropes. Specifically, we chose one member from each of the families under consideration. The structures studied included poly-spiro[8]carbon, poly-0-bi(cyclo[8]carbon), poly-1-bi(cyclo[8]carbon), and poly-0-fused[8]carbon. To model an isolated one-dimensional system, we created a slab in the non-periodic directions of 17.0 Å. This value was established after convergence tests, presented in the SI section.
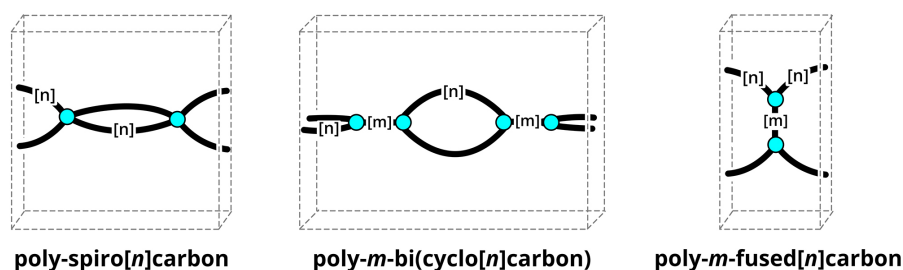
The structure of poly-spiro[8]carbon is presented in Figure 5a, showing a tetragonal unit cell with cell parameters along the periodic axis being z = 20.15 Å. The optimized structure presented a D_{2h} point group symmetry, the same as its molecular analogue. The carbine arches moiety connected by the sp^3 carbon atoms presented polyynic behavior, with bond lengths of 1.22 and 1.34 Å, resulting in a BLA of 0.107 Å. The poly-0-fused[8]carbon, presented in Figure 5b, possesses a tetragonal unit cell with the parameter along the periodic axis of x = 11.17 Å. The optimized structure presented a D_{2h} point group symmetry, as in its molecular analogue. The carbine arc moiety presented a polyynic behavior, with bond lengths of 1.332 and 1.234 Å, resulting in a BLA of 0.092 Å.

The poly-0-bi(cyclo[8]carbon) is presented in Figure 5c, in a tetragonal unit cell with the parameter along the periodic axis being x = 11.07 Å. The optimized structure presented a D_{2h} point group symmetry, as in its molecular analogue. The carbine arc moiety presented a polyynic behavior, with bond lengths of 1.393 and 1.244 Å, resulting in a BLA of 0.109. The poly-1-bi(cyclo[18]carbon) presents six non-equivalent atoms, as shown in Figure 5d, in a tetragonal cell with D_{2h} point group symmetry and z = 24.88 Å. The carbine arches moiety also presented a polyynic configuration with bond lengths of 1.23 and 1.33 Å, resulting in a BLA of 0.985 Å.

The poly-spiro[8]carbon molecule exhibits a sp^3 carbon atom connecting the carbine arches. This restricts the conjugation between the π-bonds in the structure leading to an increase in the band gap and a reduction in the band's dispersion, as illustrated in Figure 6a. Similarly, the poly-1-bi(cyclo[8]carbon) molecule displays a behavior whereby the carbon atom that joins the cyclic moieties forms a cumulenic double bond, also impeding the conjugation between these units. As a result, the band gap is increased, and the band dispersion is reduced, as depicted in Figure 6d.

In structures such as poly-0-fused[8]carbon and poly-0-bi(cyclo[8]carbon), the conjugation of π-bonds remains possible, thereby reducing the band gap and increasing the band dispersion near the Fermi level. Notably, the poly-*m*-bi(cyclo[*n*]carbons) with *m* = 1 exhibited a bandgap of

| poly-*spiro*[*n*]carbon | poly-*m*-bi(cyclo[*n*]carbon) | poly-*m*-fused[*n*]carbon |

Figure 4. Scheme representing the topology of the new proposed 1D-periodic carbon allotropes. The [*m*] and [*n*] represent the number of carbon atoms on the respective sections of each structure while the blue circles represent the carbon atoms that form the connection between the carbine sections.
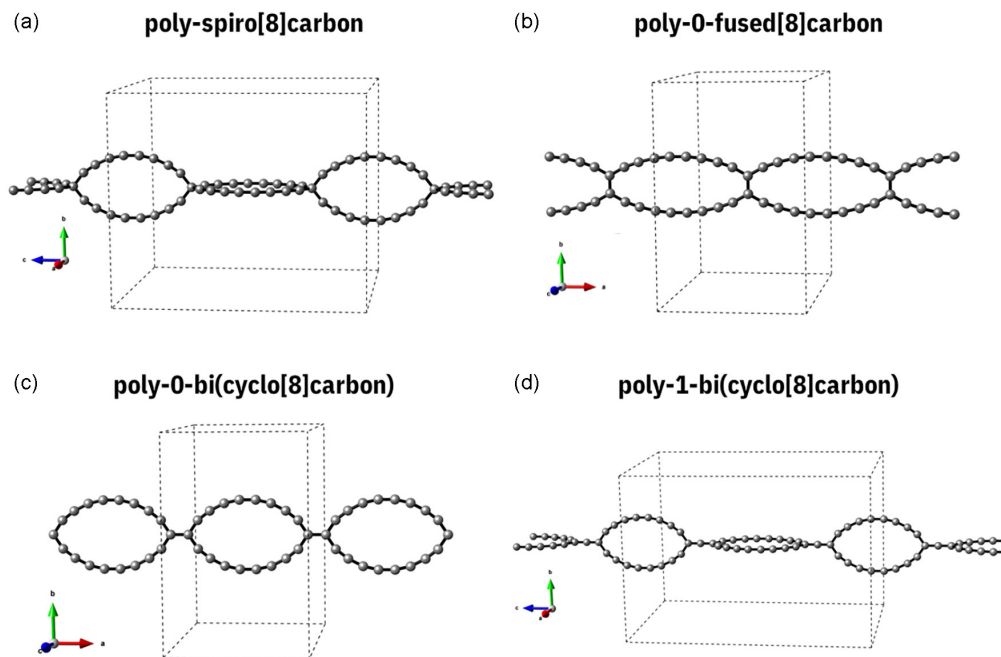
Figure 5. Atomic representation of poly-spiro[8]carbon (a), poly-0-fused[8]carbon (b), poly-0-bi(cyclo[8]carbon) (c), and poly-1-bi(cyclo[8]carbon) (d).
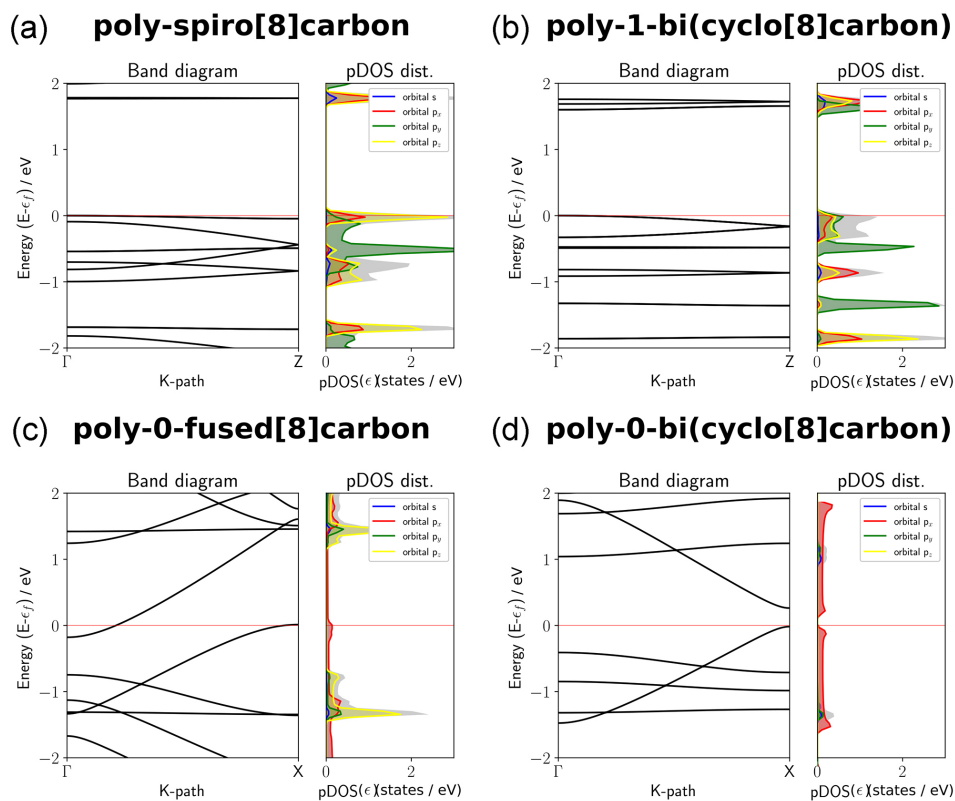

Figure 6. Band diagram and projected density of states (pDOS) of the proposed 1D carbon allotropes. The Fermi energy was adjusted to zero.

1.7 eV, while with $m = 0$, the bandgap decreased to 0.5 eV at the PBE-D3(BJ) level. The poly-0-fused[8]carbon structure exhibits a unique electronic property that resembles that of a semi-metal, where the maximum of the valence band presents higher energy than the minimum of the conduction band but without intersection. Its electronic structure is characterized by a direct bandgap of 1.3 eV, however, it has a zero indirect band gap at the PBE-D3 level, making it an intriguing candidate for potential applications in electronic and optoelectronic devices.

The phonon dispersions and vibrational density of states (vDOS) for all periodic structures are presented in Figures S43-46 (SI section). The poli-0-fused[8]carbon and poli-0-bi(cyclo[8]carbon) structures are dynamically stable, with no imaginary phonon mode present in the dispersion. The poly-1-bicyclo[8]carbon and poly-spiro[8] carbon structures did not present imaginary phonons at Γ, however, they did show small imaginary modes at **X**. Nonetheless, the small values of these imaginary modes (around 15 cm^{-1}) could be attributed to numerical error due to the size of the supercell used.

Subsequently, we investigate the variation in the bandgap of the proposed allotropes when subjected to uniform strain (ε) along the periodic axis, with a range of −5% ≤ ε ≤ 5%. Figure 7 shows the relationship between the cohesive energy, bandgap, and stress as a function of the strain for the four periodic structures. The results demonstrate that each material has a distinctive electronic response.

The bandgap of poly-0-fused[8]carbon initially showed a small decrease from 0.03 eV at ε = −5% to 0.01 eV at ε = 0%, followed by an increase to 0.25 eV at ε = 5%. Conversely, poly-1-bi(cyclo[8]carbon) experienced an increase in bandgap from 1.55 eV at ε = −5% to 1.61 eV at ε = 2%, before subsequently dropping to 1.48 eV at ε = 5%.

In comparison, poly-0-bi(cyclo[8]carbon) was found to experience a comparatively smaller decrease in its bandgap, from 0.74 to 0.70 eV, which represents a variation of approximately 5%. On the other hand, poly-spiro[8]carbon exhibits a significant decrease in its bandgap, from 1.95 eV at ε = −5% to 1.5 eV at ε = 5%, representing a variation of approximately 23%. These results suggest that poly-spiro[8]carbon's significant bandgap modulation under strain could make it valuable for various applications such as optoelectronics, flexible electronics, strain sensors, and stretchable electronic devices.

Potential synthetic routes

Possible synthetic routes to obtain archicarbons can follow the strategies for preparing cyclo[18]carbon, which has already been demonstrated to be viable.[28,41] These strategies usually employ Glaser-Hay coupling,[42] in which synthetic precursors, usually based on squaric acid derivatives, are coupled, then deprotected to generate the carbonyl derivative. This would then be deposited on a surface, usually NaCl on copper, where an atomic force microscopy (AFM) tip can be used to promote CO loss, progressively leading to the desired archicarbon. An example of synthesis strategy for one of the archicarbons (a *m*-bi(cyclo[*n*]carbon, *m* = 0, *n* = 9) is shown in Figure 8. Potential synthetic routes for the other molecular and periodic archicarbons can be found in the SI section.

To guide future synthetic efforts of the proposed allotropes, SI section presents the simulated infrared and Raman spectra for the molecular models, along with the complete assignment of selected peaks and corresponding displacement vectors.

Conclusions

In conclusion, our study has delved into the intriguing realm of molecular and periodic archicarbon based on carbine arches. The exploration of diverse architectures in molecular archicarbons revealed new stable structures with polyynic configuration and distinct topologies. The investigation was extended to propose new 1D-periodic structures inspired by some of the molecular prototypes. Most of the proposed molecular archicarbons showed greater stability than cyclo[18]carbon, except for bicyclo[8]carbon, which means they may be viable. Periodic archicarbons also displayed polyynic configurations and interesting electronic properties, particularly the poly-0-fused[8]carbon. Analysis of the allotropes under
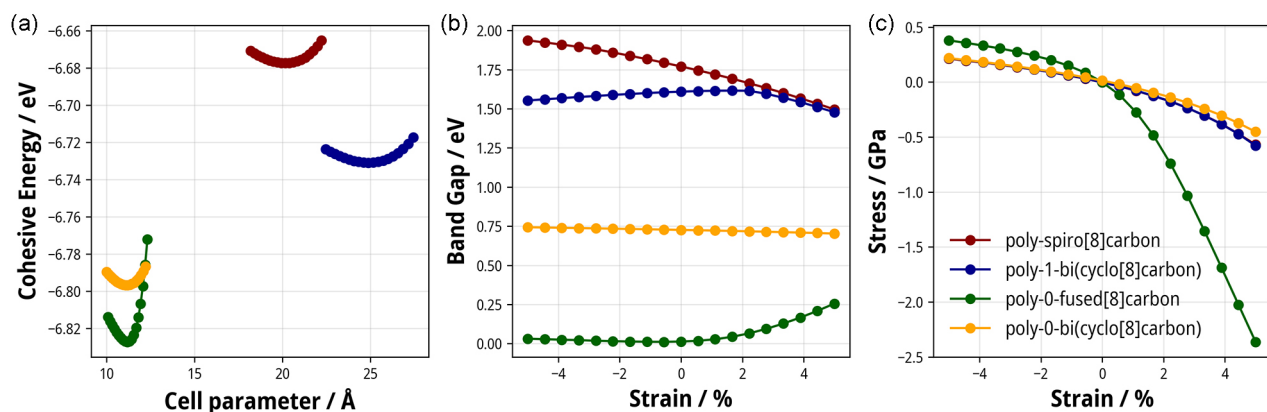

Figure 7. (a) Change of cohesive energy, (b) bandgap, and (c) stress under uniform strain of the proposed 1D carbon allotropes.
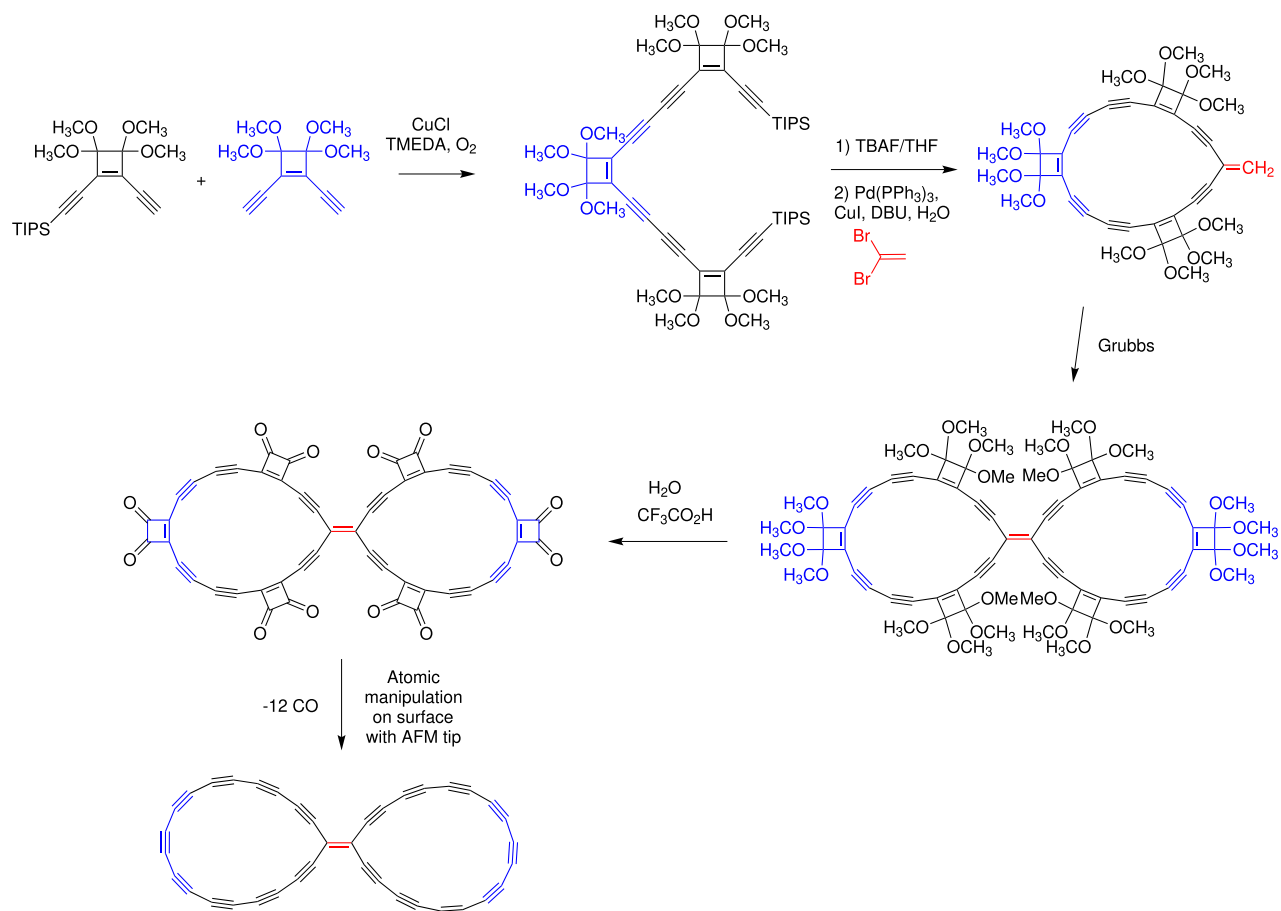
Figure 8. Example of synthetic route for the *m*-bi(cyclo[*n*]carbon).

uniform strain revealed modifications in band-gap values, especially for spiro[8]carbon, enhancing their potential for electronic applications. These exquisite carbon forms may be an open door for further adventures in the structural chemistry of carbon systems.

Supplementary Information

Supplementary information (validation of the DFT results, simulated infrared and Raman spectra of the molecular allotropes, and additional technical details (cutoff energy, *k*-point, and slab convergence) for the calculations using periodic boundary conditions, potential synthetic routes aiming the preparation of the various archicarbons) is available free of charge at http://jbcs.sbq.org.br. as PDF file. Raw output files are available on Zenodo at https://zenodo.org/records/10905716.

Acknowledgments

References

1. Diederich, F.; Kivala, M.; *Adv. Mater.* **2010**, *22*, 803. [Crossref]

2. Akinwande, D.; Huyghebaert, C.; Wang, C.-H.; Serna, M. I.; Goossens, S.; Li, L.-J.; Wong, H.-S. P.; Koppens, F. H. L.; *Nature* **2019**, *573*, 507. [Crossref]

3. Shapira, P.; Gök, A.; Salehi, F.; *J. Nanopart. Res.* **2016**, *18*, 269. [Crossref]

4. Krätschmer, W.; Lamb, L. D.; Fostiropoulos, K.; Huffman, D. R.; *Nature* **1990**, *347*, 354. [Crossref]

5. Iijima, S.; *Nature* **1991**, *354*, 56. [Crossref]

6. Novoselov, K. S.; Geim, A. K.; Morozov, S. V.; Jiang, D.; Zhang, Y.; Dubonos, S. V.; Grigorieva, I. V.; Firsov, A. A.; *Science* **2004**, *306*, 666. [Crossref]

7. Tiwari, S. K.; Kumar, V.; Huczko, A.; Oraon, R.; de Adhikaro, A.; Nayak, G. C.; *Crit. Rev. Solid State Mater. Sci.* **2016**, *41*, 257. [Crossref]

8. Castro Neto, A. H.; *Mater. Today* **2010**, *13*, 12. [Crossref]

9. Nguyen, A. L.; Liu, W.; Khor, K. A.; Nanetti, A.; Cheong, S. A.; *J. Informetr.* **2020**, *14*, 101067. [Crossref]

10. Reiss, T.; Hjelt, K.; Ferrari, A. C.; *Nat. Nanotechnol.* **2019**, *14*, 907. [Crossref]

11. Diederich, F.; Rubin, Y.; Knobler, C. B.; Whetten, R. L.; Schriver, K. E.; Houk, K. N.; Li, Y.; *Science* **1989**, *245*, 1088. [Crossref]

12. Arulmozhiraja, S.; Ohno, T.; *J. Chem. Phys.* **2008**, *128*, 114301. [Crossref]

13. Torelli, T.; Mitas, L.; *Phys. Rev. Lett.* **2000**, *85*, 1702. [Crossref]

14. Parasuk, V.; Almlof, J.; Feyereisen, M. W.; *J. Am. Chem. Soc.* **1991**, *113*, 1049. [Crossref]

15. Neiss, C.; Trushin, E.; Görling, A.; *ChemPhysChem* **2014**, *15*, 2497. [Crossref]

16. Martin, J. M. L.; El-Yazal, J.; François, J.-P.; *Chem. Phys. Lett.* **1995**, *242*, 570. [Crossref]

17. Pereira, Z. S.; da Silva, E. Z.; *J. Phys. Chem. A* **2020**, *124*, 1152. [Crossref]

18. Baryshnikov, G. V; Valiev, R. R.; Kuklin, A. V; Sundholm, D.; Ågren, H.; *J. Phys. Chem. Lett.* **2019**, *10*, 6701. [Crossref]

19. Fowler, P. W.; Mizoguchi, N.; Bean, D. E.; Havenith, R. W. A.; *Chem. - Eur. J.* **2009**, *15*, 6964. [Crossref]

20. Remya, K.; Suresh, C. H.; *RSC Adv.* **2016**, *6*, 44261. [Crossref]

21. Saito, M.; Okamoto, Y.; *Phys. Rev. B* **1999**, *60*, 8939. [Crossref]

22. Kaiser, K.; Scriven, L. M.; Schulz, F.; Gawel, P.; Gross, L.; Anderson, H. L.; *Science* **2019**, *365*, 1299. [Crossref]

23. Hutter, J.; Luethi, H. P.; Diederich, F.; *J. Am. Chem. Soc.* **1994**, *116*, 750. [Crossref]

24. Fedik, N.; Kulichenko, M.; Steglenko, D.; Boldyrev, A. I.; *Chem. Commun.* **2020**, *56*, 2711. [Crossref]

25. Baryshnikov, G. V.; Valiev, R. R.; Nasibullin, R. T.; Sundholm, D.; Kurten, T.; Ågren, H.; *J. Phys. Chem. A* **2020**, *124*, 10849. [Crossref]

26. Sun, L.; Zheng, W.; Gao, W.; Kang, F.; Zhao, M.; Xu, W.; *Nature* **2023**, *623*, 972. [Crossref]

27. Albrecht, F.; Ronc, I.; Gao, Y.; Paschke, F.; Baiardi, A.; Tavernelli, I.; Mishra, S.; Anderson, H. L.; Gross, L.; *ChemRxiv*, 2024. [Crossref] accessed in July 2024

28. Gao, Y.; Albrecht, F.; Rončević, I.; Ettedgui, I.; Kumar, P.; Scriven, L. M.; Christensen, K. E.; Mishra, S.; Righetti, L.; Rossmannek, M.; Tavernelli, I.; Anderson, H. L.; Gross, L.; *Nature* **2023**, *623*, 977. [Crossref]

29. Frisch, M. J.; Trucks, G. W.; Schlegel, H. B.; Scuseria, G. E.; Robb, M. A.; Cheeseman, J. R.; Scalmani, G.; Barone, V.; Petersson, G. A.; Nakatsuji, H.; Li, X.; Caricato, M.; Marenich, A. V.; Bloino, J.; Janesko, B. G.; Gomperts, R.; Mennucci, B.; Hratchian, H. P.; Ortiz, J. V.; Izmaylov, A. F.; Sonnenberg, J. L.; Williams-Young, D.; Ding, F.; Lipparini, F.; Egidi, F.; Goings, J.; Peng, B.; Petrone, A.; Henderson, T.; Ranasinghe, D.; Zakrzewski, V. G.; Gao, J.; Rega, N.; Zheng, G.; Liang, W.; Hada, M.; Ehara, M.; Toyota, K.; Fukuda, R.; Hasegawa, J.; Ishida, M.; Nakajima, T.; Honda, Y.; Kitao, O.; Nakai, H.; Vreven, T.; Throssell, K.; Montgomery Jr., J. A.; Peralta, J. E.; Ogliaro, F.; Bearpark, M. J.; Heyd, J. J.; Brothers, E. N.; Kudin, K. N.; Staroverov, V. N.; Keith, T. A.; Kobayashi, R.; Normand, J.; Raghavachari, K.; Rendell, A. P.; Burant, J. C.; Iyengar, S. S.; Tomasi, J.; Cossi, M.; Millam, J. M.; Klene, M.; Adamo, C.; Cammi, R.; Ochterski, J. W.; Martin, R. L.; Morokuma, K.; Farkas, O.; Foresman, J. B.; Fox, D. J.; *Gaussian 16, Revision A.03*, Gaussian, Inc., Wallingford CT, 2016.

30. *Quantum Espresso*, version 6.8, Quantum ESPRESSO Foundation (QEF), 2021 [Link] accessed in July 2024; Giannozzi, P.; Baroni, S.; Bonini, N.; Calandra, M.; Car, R.; Cavazzoni, C.; Ceresoli, D.; Chiarotti, G. L.; Cococcioni, M.; Dabo, I.; Dal Corso, A.; de Gironcoli, S.; Fabris, S.; Fratesi, G.; Gebauer, R.; Gerstmann, U.; Gougoussis, C.; Kokalj, A.; Lazzeri, M.; Martin-Samos, L.; Marzari, N.; Mauri, F.; Mazzarello, R.; Paolini, S.; Pasquarello, A.; Paulatto, L.; Sbraccia, C.; Scandolo, S.; Sclauzero, G.; Seitsonen, A. P.; Smogunov, A.; Umari, P.; Wentzcovitch, R. M.; *J. Phys.: Condens. Matter* **2009**, *21*, 395502. [Crossref]

31. Giannozzi, P.; Andreussi, O.; Brumme, T.; Bunau, O.; Buongiorno Nardelli, M.; Calandra, M.; Car, R.; Cavazzoni, C.; Ceresoli, D.; Cococcioni, M.; Colonna, N.; Carnimeo, I.; Dal Corso, A.; de Gironcoli, S.; Delugas, P.; DiStasio, R. A.; Ferretti, A.; Floris, A.; Fratesi, G.; Fugallo, G.; Gebauer, R.; Gerstmann, U.; Giustino, F.; Gorni, T.; Jia, J.; Kawamura, M.; Ko, H.-Y.; Kokalj, A.; Küçükbenli, E.; Lazzeri, M.; Marsili, M.; Marzari, N.; Mauri, F.; Nguyen, N. L.; Nguyen, H.-V.; Otero-de-la-Roza, A.; Paulatto, L.; Poncé, S.; Rocca, D.; Sabatini, R.; Santra, B.; Schlipf, M.; Seitsonen, A. P.; Smogunov, A.; Timrov, I.; Thonhauser, T.; Umari, P.; Vast, N.; Wu, X.; Baroni, S.; *J. Phys.: Condens. Matter* **2017**, *29*, 465901. [Crossref]

32. Peverati, R.; Truhlar, D. G.; *J. Phys. Chem. Lett.* **2011**, *2*, 2810. [Crossref]

33. Goerigk, L.; Grimme, S.; *J. Chem. Theory Comput.* **2011**, *7*, 291. [Crossref]

34. Perdew, J. P.; Burke, K.; Ernzerhof, M.; *Phys. Rev. Lett.* **1996**, *77*, 3865. [Crossref]

35. Vanderbilt, D.; *Phys. Rev. B* **1990**, *41*, 7892. [Crossref]

36. Monkhorst, H. J.; Pack, J. D.; *Phys. Rev. B* **1976**, *13*, 5188. [Crossref]

37. Pfrommer, B. G.; Côté, M.; Louie, S. G.; Cohen, M. L.; *J. Comput. Phys.* **1997**, *131*, 233. [Crossref]

38. Blöchl, P. E.; Jepsen, O.; Andersen, O. K.; *Phys. Rev. B* **1994**, *49*, 16223. [Crossref]

39. Togo, A.; *J. Physical. Soc. Japan* **2023**, *92*, 012001. [Crossref]

40. Togo, A.; Chaput, L.; Tadano, T.; Tanaka, I.; J. Phys.: *Condens. Matter* **2023**, *35*, 353001. [Crossref]

41. Scriven, L. M.; Kaiser, K.; Schulz, F.; Sterling, A. J.; Woltering, S. L.; Gawel, P.; Christensen, K. E.; Anderson, H. L.; Gross, L.; *J. Am. Chem. Soc.* **2020**, *142*, 12921. [Crossref]

42. Hay, A. S.; *J. Org. Chem.* **1962**, *27*, 3320. [Crossref]